Available online at www.sciencedirect.com
ScienceDirect
European Journal of Pharmaceutics and Biopharmaceutics 65 (2007) 26–38
European Journal of Pharmaceutics and Biopharmaceutics
www.elsevier.com/locate/ejpb

Research paper

Studies on dissolution enhancement and mathematical modeling of drug release of a poorly water-soluble drug using water-soluble carriers

Naveen Ahuja, Om Prakash Katare, Bhupinder Singh *

University Institute of Pharmaceutical Sciences, Panjab University, Chandigarh, India

Received 11 March 2006; accepted in revised form 13 July 2006
Available online 20 July 2006

Abstract

Role of various water-soluble carriers was studied for dissolution enhancement of a poorly soluble model drug, rofecoxib, using solid dispersion approach. Diverse carriers *viz*. polyethylene glycols (PEG 4000 and 6000), polyglycolized fatty acid ester (Gelucire® 44/14), polyvinylpyrollidone K25 (PVP), poloxamers (Lutrol® F127 and F68), polyols (mannitol, sorbitol), organic acid (citric acid) and hydrotropes (urea, nicotinamide) were investigated for the purpose. Phase-solubility studies revealed A_L type of curves for each carrier, indicating linear increase in drug solubility with carrier concentration. The sign and magnitude of the thermodynamic parameter, Gibbs free energy of transfer, indicated spontaneity of solubilization process. All the solid dispersions showed dissolution improvement vis-à-vis pure drug to varying degrees, with citric acid, PVP and poloxamers as the most promising carriers. Mathematical modeling of *in vitro* dissolution data indicated the best fitting with Korsemeyer–Peppas model and the drug release kinetics primarily as Fickian diffusion. Solid state characterization of the drug–poloxamer binary system using XRD, FTIR, DSC and SEM techniques revealed distinct loss of drug crystallinity in the formulation, ostensibly accounting for enhancement in dissolution rate.

Keywords: BCS Class II; Rofecoxib; Bioavailability; Dissolution; Polyethylene glycol; Gelucire; Polyols; Hydrotrope; Poloxamer; Release kinetics

1. Introduction

Poorly water-soluble drugs are associated with slow drug absorption leading eventually to inadequate and variable bioavailability [1,2]. And nearly 40% of the new chemical entities currently being discovered are poorly water-soluble drugs [3,4]. Based upon their permeability characteristics, the Biopharmaceutics classification system (BCS) categorizes such drugs in two major classes, i.e., Class II and IV [1,5]. The BCS class II drugs are poorly water-soluble entities with high permeability. Attempts to enhance drug solubility of these therapeutic agents correlate well with enhancement in their bioavailability [1,2,5]. Most formulation strategies for such drugs are targeted at enhancing their dissolution rate and/or solubility *in vivo* by achieving their fine dispersion at absorption level [2,6,7]. This can be attained by formulating supersaturated systems (i.e., solid dispersion) of the drug employing diverse types of carriers, ranging widely from water-soluble to amphiphilic to lipid-soluble ones [2,8–10].

Rofecoxib (RFX), chosen in the current studies, is a poorly water-soluble drug known to demonstrate dissolution or solubility limited absorption [11,12]. Although the mean bioavailability of the drug is 93%, yet its rate of absorption is quite inconsistent and delayed with t_{max} ranging from 2 to 9 h. Based upon its aqueous solubility and various dissolution parameters, the drug bioavailability can unambiguously be regarded as limited solely to dissolution. Of late, a few attempts to enhance the solubility and/or dissolution of RFX have appeared in the literature using carriers like urea, polyethylene glycol 4000 and

* Corresponding author. University Institute of Pharmaceutical Sciences, Panjab University, Chandigarh 160014, India. Tel.: +91 172 2534103; fax: +91 172 2541142.
E-mail address: bsbhoop@yahoo.com (B. Singh).

0939-6411/$ - see front matter © 2006 Elsevier B.V. All rights reserved.
doi:10.1016/j.ejpb.2006.07.007

cyclodextrins, and solvent systems like ethanol–water and ethanol–glycerol [13–17]. Besides investigating the role of diverse water-soluble carriers in improvement of solubility/dissolution of RFX, the current studies aim at exploring the mechanism of drug release through mathematical modeling of dissolution data for all the studied drug–carrier binary systems and solid state characterization of the most promising one. Albeit the drug has lately been withdrawn from the market, the results obtained for the solubility and dissolution enhancement of this model drug can be rationally extrapolated to other poorly soluble therapeutic agents too.

2. Materials and methods

2.1. Materials

Rofecoxib (RFX) was procured *ex-gratis* from M/s Unichem Ltd., Mumbai, India. Lutrol® F127 and Lutrol® F68, and Gelucires® were obtained as gift samples from M/s BASF, Bangalore, India, and M/s Gattefosse (Cedex, France), respectively. All other chemicals used were of analytical grade.

2.2. Preparation of solid dispersions and corresponding physical mixtures

Solid dispersions (1.5 g) were prepared employing various water-soluble carriers *viz.* polyethylene glycols (PEG 4000 and PEG 6000), polyglycolized fatty acid ester (Gelucire® 44/14), poloxamers (Lutrol® F127 and Lutrol® F68), polyols (mannitol, sorbitol), organic acid (citric acid), and hydrotropes (urea and nicotinamide) by hot-melt method. Each carrier was melted over a thermostatically controlled magnetic stirrer at its respective melting point and drug was incorporated into the molten carrier mass. The blend was heated at the corresponding temperature for 5 min, followed by flash-cooling on an ice bath. The dispersions with polyvinyl pyrollidone (PVP K25), however, were prepared by solvent evaporation technique (45 °C) under vacuum using methanol/chloroform (2:1 v/v) as the solvent mixture. Each solid dispersion batch was prepared in duplicate employing each carrier in three proportions, i.e., 50%, 75% and 90% w/w. The dispersions were subsequently desiccated under vacuum for 48 h and sieved (300 μ). The physical mixtures of drug and the most promising carrier were also prepared by blending them by trituration for 10 min followed with sieving (300 μ).

2.3. Phase-solubility studies

Solubility measurements were performed in triplicate using the method reported by Higuchi and Connors [18]. An excess amount of RFX was added to the aqueous solutions of each carrier in simulated intestinal fluid (SIF, USP XXIII) containing increasing concentrations of the individual carrier (i.e., 0.1%, 0.25%, 0.5%, 0.75% and 1% w/v). The flasks were sealed and shaken at 37 °C for 48 h in a thermostatically controlled water bath and the samples were filtered through a 0.45 μm cellulose nitrate membrane filter. The filtrate was suitably diluted and analyzed spectrophotometrically (Shimadzu 1601, Japan) at 267 nm.

2.4. In vitro dissolution studies

Drug release studies were performed in triplicate on dissolution test apparatus (M/s LabIndia, Mumbai, India) at 37 ± 0.5 °C employing USP apparatus II at 100 rpm. SIF without enzyme (1000 mL) with 1% sodium lauryl sulphate (SLS) was employed as the dissolution medium. Dissolution studies were performed on pure drug (25 mg) and the solid dispersions containing an equivalent amount of the drug. Aliquots of the periodically withdrawn samples (5 mL) were analyzed spectrophotometrically at 267 nm, and were replaced with an equal volume of plain dissolution medium.

2.5. Powder X-ray diffraction studies

Powder X-ray diffraction (PXRD) patterns were traced employing X-ray diffractometer (Philips PW 1729) for the samples, using Ni filtered CuK (∝) radiation, a voltage of 35 kV, a current of 20 mA and receiving slit of 0.2 in. The samples were analyzed over 2θ range of 2–40° with scan step size of 0.020° (2θ) and scan step time of 1 s.

2.6. Differential scanning calorimetric studies

Differential scanning calorimetric (DSC) analyses of the drug, carrier, solid dispersion formulation and its corresponding physical mixture were carried out on the samples using DSC-821e (Mettler Toledo, Switzerland). Samples (6.5–10.9 mg) were heated under nitrogen atmosphere on an aluminum pan at a rate of 10 °C/min over the temperature range of 5 and 300 °C. Thermal data analyses of DSC thermograms were conducted using STAR^e software (Version 5.21).

2.7. Fourier transform infra red spectroscopy

Fourier transform infrared (FT-IR) spectroscopy was employed to further characterize the possible interactions between the drug and the carrier in the solid state on an FT-IR multiscope spectrophotometer (Perkin-Elmer, Buckinghamshire, UK) by the conventional KBr pellet method. The spectra were scanned over a frequency range 4000–500 cm^{-1} with a resolution of 4 cm^{-1}.

2.8. Scanning electron microscopy (SEM)

Samples of pure drug, carrier, the solid dispersion formulation and the corresponding physical mixture were mounted onto the stubs using double-sided adhesive tape and then coated with gold palladium alloy (150–200 Å)

using fine coat ion sputter (Jeol, fine coat ion sputter, JFC-1100). The samples were subsequently analyzed under the scanning electron microscope (JSM 6100, Jeol, Japan) for external morphology.

2.9. Data analysis

2.9.1. Phase-solubility studies

The values of apparent stability constant, K_s, between each drug–carrier combination were computed from the phase-solubility profiles, as described below:

$$K_s = \frac{\text{slope}}{\text{intercept}(1 - \text{slope})} \tag{1}$$

The values of Gibbs free energy of transfer, ΔG^{o}_{tr}, of RFX from plain SIF to aqueous solution of the carriers were calculated according to the following relationship:

$$\Delta G^{o}_{tr} = -2.303RT \cdot \log \frac{S_o}{S_s} \tag{2}$$

where, S_o and S_s are the molar solubilities of RFX in 1% w/v aqueous solution of the carrier and in the plain SIF, respectively.

2.9.2. In vitro dissolution data

Drug release data were appropriately corrected for losses of drug and dissolution medium volume during sampling by replacement using the following equation [19]:

$$C_i = A_i\left(\frac{V_s}{V_t}\right) \cdot \sum_{i=1}^{n-1} A_i\left[\frac{V_t}{(V_t - V_s)}\right] \tag{3}$$

where, C_i is the corrected absorbance of i^{th} observation, A_i is the observed specific absorbance, V_s is the sample volume, and V_t is the total volume of dissolution medium.

The values of $t_{85\%}$ and $t_{90\%}$ were calculated using Stineman interpolation option of the GRAPH (MicroMath Inc., USA) software (Version 2.0).

Percent dissolution efficiency (%DE) was also computed to compare the relative performance of various carriers in solid dispersion formulations [20]. The magnitude of %DE at 10 min ($\%DE_{10\ min}$) and 30 min ($\%DE_{30\ min}$) for each formulation was computed as the percent ratio of area under the dissolution curve up to the time, t, to that of the area of the rectangle described by 100% dissolution at the same time.

$$\%DE = \left(\frac{\int_0^t y \cdot dt}{y_{100} \cdot t}\right)100 \tag{4}$$

2.9.2.1. Mathematical modeling of release kinetics. The *in vitro* drug release data were fitted to various release kinetic models [8,21–23] *viz*. first-order, Higuchi, Hixson-Crowell cube root, Korsemeyer–Peppas and zero-order model employing the following set of equations:

First-order model

$$\ln(M_o/M_t) = k_1 t \tag{5}$$

Zero-order kinetic model

$$M_o - M_t = k_o t \tag{6}$$

Higuchi model

$$M_t = K\sqrt{t} \tag{7}$$

Hixson-Crowell cube root model

$$(W_o)^{1/3} - (W_t)^{1/3} = k_{1/3} t \tag{8}$$

Korsemeyer–Peppas model

$$\frac{M_t}{M_\infty} = kt^n \tag{9}$$

where, M_o, M_t and M_∞ correspond to the drug amount taken at time equal to zero, dissolved at a particular time, t, and at infinite time, respectively. The terms W_o and W_t refer to the weight of the drug taken initially and at time t, respectively. Various other terms *viz*. k, k_o, k_1, $k_{1/3}$ and K refer to the release kinetic constants obtained from the linear curves of Korsemeyer–Peppas, zero-order, first-order, Hixson-Crowell cube root law and Higuchi model, respectively. Model fitting using Eqs. (5)–(9) was accomplished using the advanced version of ZOREL software [24].

3. Results and discussion

3.1. Phase-solubility studies

Solubility of RFX in SIF was observed to be 8.9 μg mL^{-1} indicating it as practically insoluble in SIF. Various parameters computed from the phase-solubility studies (Table 1) show a linear increase in drug solubility with increased carrier levels, with r^2 values varying between 0.9084 and 0.9996. Analogous results have been reported with several other drugs using the water-soluble carriers, attributable to the formation of weakly soluble complexes [13,25–28] and/or cosolvent effect of the carrier [29]. Hydrophilic carriers are known to interact with drug molecules mainly by electrostatic forces and occasionally by other types of forces like hydrogen bonds [30].

In general, the solubility enhancement of RFX obtained with various carriers followed the rank order of surfactant ≫ organic acid ≫ polymers > hydrotropes > polyols. Taking the values of slopes of the various linear curves, enlisted in Table 1, as indicative of the relative solubilizing efficiency, the poloxamers (L127 > L68) had the maximum solubilizing power, followed by citric acid (CA) > PVP K25 > urea (UR) > PEG 4000 > PEG 6000 > mannitol (Mann) > sorbitol (Sorb) > nicotinamide (NA). Liu et al. however have reported slightly different order of solubility enhancement of RFX using various carriers in water, i.e., UR > PVP K30 > PEG 4000 > Mann [15]. Relatively higher drug solubility observed with PVP vis-à-vis UR by us can be explained as due to the difference in the PVP grade

Table 1
Solubility parameters of RFX obtained with various carriers at 37 °C

Carrier (1% w/v)	Slope	Stability constant (mL g^{-1})	r^2
Organic acid			
Citric acid	1.16×10^{-3}	130.38	0.9928
Hydrotropes			
Urea	6.23×10^{-4}	62.04	0.9084
Nicotinamide	1.43×10^{-4}	16.25	0.9895
Polyols			
Sorbitol	2.89×10^{-4}	32.48	0.9978
Mannitol	3.28×10^{-4}	37.54	0.9811
Polymers			
PEG 4000	4.25×10^{-4}	46.98	0.9902
PEG 6000	3.78×10^{-4}	43.46	0.9874
PVP K25	7.82×10^{-4}	87.94	0.9983
Surfactants			
Lutrol® F127	3.05×10^{-2}	4618.04	0.9996
Lutrol® F68	1.45×10^{-2}	1806.72	0.9964

PEG, polyethylene glycol; PVP, polyvinylpyrollidone.

and nature of the solvent employed (i.e., SIF) in the current studies.

The values of apparent stability constant, K_s, were computed for 1:1 drug–carrier interactions (Table 1) since all the curves obtained in the present studies were of A_L type with the resultant slopes as less than unity [18]. Highest values of K_s obtained for poloxamer binary solutions revealed strong binding affinity between RFX and the solubilizer. At 1% w/v concentration of the carriers, L127 and L68 showed 35.3- and 17.5-fold augmentation in the solubility of pure drug, attributable to the micellar solubilization of drug [31]. Besides poloxamers, the other water-soluble polymeric carriers, i.e., PVP, PEG 4000 and PEG 6000 also enhanced RFX solubility although moderately.

Further, Table 2 shows that all the values of ΔG^{o}_{tr} were negative at all the levels of carriers, unequivocally demonstrating spontaneity of drug solubilization process. The values show a declining trend with increase in the carrier concentration too construing that the process of RFX transfer from plain SIF to carrier solution is more favourable at higher carrier levels. The values of ΔG^{o}_{tr} were the lowest for L127 indicating that the process of transfer of RFX from plain SIF to its aqueous solutions was most favourable amongst all the carriers studied.

3.2. In vitro dissolution studies

Drug release studies on poorly water-soluble drugs often require dissolution media encompassing small amounts of surfactants or solvents to provide sink conditions for dissolution of poorly soluble drugs [32–34]. The use of surfactants in the dissolution systems has physiological significance too as natural surfactants like bile salts are usually present in the gastrointestinal tract. The ability of surfactants to accelerate *in vitro* dissolution of poorly water-soluble drugs has been attributed to wetting, micellar solubilization, and/or deflocculation [33]. Accordingly, the current dissolution studies on RFX and the RFX–carrier systems were carried out in a surfactant-based dissolution medium, i.e., SIF with 1.0% w/v SLS. Further, the visual observation also revealed the tendency of the drug to leave the surface of the dissolution medium instantaneously and disperse in the bulk of the medium indicating its rapid wetting. However, no similar impregnation of drug could be noted in the aqueous medium without surfactant.

3.2.1. Effect of different carriers on the dissolution of RFX from solid dispersions

Table 3 enlists the dissolution parameters of RFX solid dispersions with various carriers (CA, NA, UR, L127, L68, G44, PEG 4000, PEG 6000, PVP, Mann, and Sorb) in three concentrations of each carrier. As is evident from the Table, the dissolution rate of pure RFX is low even in the surfactant-based medium, as 85% of the drug gets dissolved in more than 1 h (69 min) and nearly 10% of the drug remains undissolved even after the entire dissolution span of 2 h.

Solid dispersions formulated with all the carriers exhibited significant improvement in the dissolution parameters of RFX. The order of dissolution enhancement with various binary systems was found to be CA ≅ L127 > PVP > L68 > UR ≅ PEG 4000 > PEG 6000 ≅ NA > G44 > Mann > Sorb. This order was not in exact consonance with that obtained during phase-solubility studies, where CA and NA showed lower solubility enhancement. Relatively higher dissolution enhancement in such cases could be credited to more intimate drug–carrier interaction in the molten state during formulation of solid dispersions. Increased dissolution of RFX from the dispersions could

Table 2
Values of Gibbs free energy of transfer, ΔG^{o}_{tr}, a thermodynamic parameter of the solubility process of rofecoxib in the aqueous solutions of various carriers

Concentration of carrier (%w/v)	ΔG^{o}_{tr} (joules/mol) for various water-soluble carriers at 37 °C									
	CA	UR	NA	Sorb	Mann	PEG 4000	PEG 6000	PVP	L127	L68
0.1	−326.05	−548.44	−31.66	−99.44	−28.80	−140.90	−57.29	−248.32	−3529.78	−2125.58
0.25	−694.09	−896.162	−57.29	−221.88	−113.33	−376.60	−168.18	−474.81	−5755.69	−4289.71
0.5	−1396.66	−1117.56	−195.17	−401.51	−413.87	−638.17	−401.51	−980.69	−7463.65	−5724.45
0.75	−1674.32	−1317.97	−274.49	−592.54	−638.17	−791.78	−713.92	−1311.01	−8405.41	−6505.04
1	−2175.88	−1477.92	−376.60	−722.69	−748.82	−1025.83	−875.62	−1622.36	−9183.13	−7382.33

CA, citric acid; UR, urea; NA, nicotinamide; Sorb, sorbitol; Mann, mannitol; PEG, polyethylene glycol; PVP, polyvinyl pyrollidone K25; L127, Lutrol® F127; L68, Lutrol® F68.

Table 3
Dissolution parameters of rofecoxib and various solid dispersion formulations

S. No.	Formulation[a]	Dissolution parameters							
		$DP_{5\ min}$[b]	$DP_{15\ min}$[b]	$DP_{120\ min}$[b]	$\%DE_{10\ min}$[c]	$\%DE_{30\ min}$[c]	$RDr_{5\ min}$[d]	$t_{85\%}$ (min)[e]	$t_{90\%}$ (min)[e]
1	Pure RFX	26.01	55.93	90.66	23.87	47.06	–	69.27	104.46
2	RCA50%	40.93	72.41	95.55	36.74	63.68	1.57	28.47	46.69
3	RCA25%	65.60	90.25	97.93	52.14	78.59	2.52	12.94	14.84
4	RCA10%	92.60	99.93	91.98[f]	71.18	89.56	3.56	04.34	04.70
5	RNA50%	32.60	59.30	93.56	28.53	51.11	1.25	68.25	91.07
6	RNA25%	36.11	64.76	98.46	31.33	56.16	1.39	48.23	65.72
7	RNA10%	49.56	76.14	100.01	42.29	70.66	1.91	18.30	21.24
8	RU50%	34.93	63.53	94.20	31.42	57.82	1.34	41.51	57.15
9	RU25%	46.26	71.80	99.13	39.26	65.24	1.78	24.64	30.31
10	RU10%	65.38	91.74	99.99	53.00	80.23	2.51	11.83	14.02
11	RL127-50%	44.62	69.02	99.86	37.16	61.35	1.72	40.78	56.24
12	RL127-25%	61.98	83.35	100.47	50.85	75.71	2.38	16.38	20.08
13	RL127-10%	89.29	98.42	100.06	68.89	88.94	3.43	04.56	05.24
14	RL68-50%	46.29	65.67	96.76	38.23	58.75	1.78	48.63	63.24
15	RL68-25%	57.05	73.06	100.10	45.02	68.42	2.19	22.80	26.93
16	RL68-10%	69.48	88.25	100.01	54.65	79.24	2.67	12.86	16.24
17	RG44-50%	16.79	46.06	92.89	17.28	40.81	0.65	70.27	88.69
18	RG44-25%	21.32	54.51	100.01	20.64	48.88	0.82	38.38	50.73
19	RG44-10%	37.58	68.39	100.33	32.86	60.25	1.45	29.48	38.29
20	RPEG4-50%	34.30	62.61	100.02	29.05	55.11	1.32	45.17	59.87
21	RPEG4-25%	39.14	67.32	100.04	32.52	59.58	1.51	28.37	37.14
22	RPEG4-10%	65.16	84.69	100.10	52.17	77.28	2.51	15.21	18.16
23	RPEG6-50%	22.54	56.14	94.71	21.72	49.41	0.87	50.17	58.05
24	RPEG6-25%	38.32	63.40	96.55	31.64	57.57	1.47	31.87	43.10
25	RPEG6-10%	55.45	80.42	97.95	45.58	71.13	2.13	18.55	30.27
26	RPVP50%	50.25	73.38	100.20	41.15	67.08	1.93	21.68	33.97
27	RPVP25%	53.86	80.18	95.35[f]	44.8	71.70	2.07	18.52	23.43
28	RPVP10%	83.84	95.30	94.87[f]	66.07	86.33	3.22	05.30	6.12
29	RMann50%	19.33	34.38	81.52	16.44	31.45	0.74	–	–
30	RMann25%	30.63	44.14	89.32	25.84	43.21	1.18	92.78	–
31	RMann10%	42.52	67.09	100.02	35.44	59.89	1.64	37.82	51.81
32	RSorb50%	27.25	45.95	89.61	23.69	41.87	1.05	103.73	–
33	RSorb25%	33.23	51.34	91.72	28.36	47.08	1.28	91.50	113.31
34	RSorb10%	45.96	63.85	95.68	37.79	58.10	1.77	51.95	66.97

[a] 50%, 25% and 10% in formulation code signify the percent drug present in the dispersion.
[b] DP: Percent drug released at particular time.
[c] %DE: Percent dissolution efficiency at particular time.
[d] *RDr: Relative dissolution rate at 5 min.
[e] $t_{85\%}$ and $t_{90\%}$: Time taken to release 85% and 90% of drug.
[f] Precipitation exhibited by the formulation.

be ascribed to the probable reduction in its particle size, wetting of the hydrophobic particles and augmentation of its solubility by the said carriers [2,8].

Among hydrotropes, relatively higher drug release enhancement was observed with UR systems vis-à-vis NA systems. The hydrotropic solubilization by the said carriers has been attributed mainly to their ability to destroy water structure, and/or to form complexes with certain drugs on the basis of π-electron donor–acceptor interaction, and/or to undergo hydrogen bonding [35–37]. The CA systems showed marked enhancement in rate as well as extent of RFX dissolution. The extent of diminution in $t_{90\%}$ values was observed to vary between minor (i.e., 2-fold) and major (i.e., 22-fold) with various levels of CA systems. The dissolution enhancement in CA systems has been reported to be due to the formation of glass dispersions associated with very high dissolution rates [38,39]. Amongst water-soluble polymers, the solubilizing efficiency ranked in the order of PVP ≫ PEG 4000 > PEG 6000. This finding may be accredited to the higher amorphizing properties of PVP than the PEG's, as reported in an earlier study [25]. Enhancement in drug dissolution performance with these polymers has been attributed to the formation of interstitial solid solutions [40]. The polyols (Mann, Sorb), however, improved the dissolution performance of the drug only marginally. Amidst surfactant-based systems, the poloxamer systems (L127 > L68) resulted in marked improvement in RFX dissolution, assignable to micellar solubilization [31]. The G44 system, known to decrease interfacial tension between the drug particles and water by microemulsification, was relatively much less efficient than poloxamers in the current studies [33,41–43].

The systems prepared with CA, L127 and PVP yielded almost similar results for dissolution enhancement, but

distinctly higher than all other carriers studied. However, the dissolution profiles of solid dispersions with CA (Fig. 1a) and PVP (Fig. 1b) showed gradual decline in the supersaturated level of RFX after 20 and 10 min, respectively. The decrease in RFX concentration in the supersaturated state could be ascribed to recrystallization of the drug, as reported with several other drugs [44–46]. On the other hand, extremely high concentration of RFX in the supersaturated state was maintained for the entire dissolution span in the case of L127 system (Fig. 1c), suggesting that the carrier could prevent its recrystallization. Such a high and sustainable solubility enhancement could be achieved by micellar solubilization and/or reduction of activity coefficient of the drug through reduction of hydrophobic interaction(s) [47,48]. These results unambiguously indicate L127 as the most appropriate solid dispersion carrier for RFX amongst all the carriers examined in the current study. The RFX-L127 physical mixtures also showed improvement in drug dissolution performance (data not shown), but significantly lower than the corresponding solid dispersions.

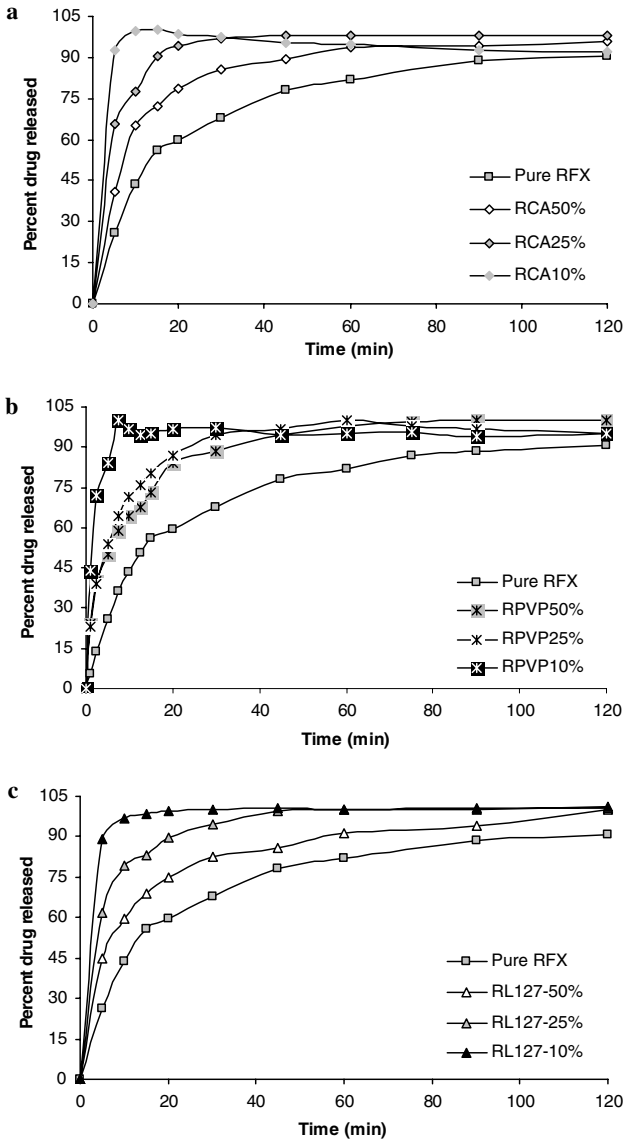

Fig. 1. Dissolution profiles of RFX–carrier binary systems: (a) citric acid systems (RCA); (b) polyvinyl pyrollidone systems (RPVP); (c) Lutrol® F127 systems (RL127); 50%, 25% and 10% correspond to the amount of RFX in the binary systems.

3.2.2. *Effect of concentration of the carriers on the dissolution of RFX from solid dispersions*

Table 3 reveals that drug dissolution improved to varying degrees with rise in the amount of each carrier. In contrast to all other explored carriers, the polyols (i.e., Mann and Sorb) at lower carrier concentrations showed rather decreased drug release rates vis-à-vis pure drug, which could be because of stronger drug–carrier interactions than drug–water and carrier–water interactions [49]. Collectively for all the carrier systems, considerable dissolution improvement was observed at the highest carrier amount, i.e., 90% w/w.

For comparative analysis of all the formulations, %DE values at two times, representing the early and late phase of dissolution study, were computed. The %DE values in the initial time period of dissolution study (e.g., $\%DE_{10\ min}$) provide comparative information for very fast releasing formulations, whereas, $\%DE_{30\ min}$ values furnish relative information about both fast and slow releasing formulations. The value of $\%DE_{10\ min}$ for pure drug (23.87) was enhanced from miniscule (32.86 for G44 system) to very high (71.18 for CA and 68.89 for L127 system) at 90% w/w carrier amount. Analogous to $\%\ DE_{10\ min}$ values, the value of $RDr_{5\ min}$ was the least for G44 system (1.45) and maximum for CA system (3.56). However, the $\%DE_{30\ min}$ values revealed the lowest dissolution improvement with Sorb system (58.10) at the same carrier level. Lower $\%DE_{10\ min}$ and $RDr_{5\ min}$ values observed with the G44 systems can probably be due to slow emulsification process leading to slower dissolution in the initial time periods (until 20 min). Maximum values of various dissolution parameters observed for CA formulation (RCA10%) construe attainment of very high rate of drug dissolution, comparable to that obtained for RL12710% formulation. Since, the high solubility of RFX from RCA10% could be retained only up to 20 min, the RL12710% formulation was considered better than this system.

3.3. *Mathematical modeling*

Table 4 enlists the regression parameters obtained after fitting various release kinetic models to the *in vitro* dissolution data. The goodness of fit for various models investigated for binary systems ranked in the order of Korsemeyer–Peppas > Higuchi ≅ first-order > Hixson-Crowell cube root law ≫ zero-order. All the kinetic models, other than the zero-order, fitted well at early time periods. Since the extent of release at given time points varied largely between inter- and intra-drug–carrier dispersions, modeling analysis was carried out by fitting the dissolution data until the time 90% of the drug was

Table 4
Statistical parameters of various formulations obtained after fitting the drug release data to various release kinetic models

S. No.	Formulation	Mathematical models for drug release kinetics									
		Higuchi		Hixson-Crowell		First-order		Korsemeyer–Peppas		Zero-order	
		Slope	r^2	Slope	r^2	Slope	r^2	Slope	r^2	Slope	r^2
1	Pure RFX	10.23	0.8241	0.0275	0.5522	−0.0105	0.7795	0.3675	0.9129	−1.07	−0.1086
2	RCA50%	16.00	0.8810	0.0697	0.6257	−0.0264	0.8017	0.3450	0.8965	−2.75	0.1907
3	RCA25%	23.25	0.9501	0.1597	0.8956	−0.0651	0.9751	0.2847	0.9828	−7.01	0.7502
4	RCA10%	30.29	0.8691	0.3297	0.8258	−0.2171	0.9948	0.0730	0.8992	−8.45	0.5127
5	RNA50%	11.43	0.8343	0.0346	0.5403	−0.0115	0.8067	0.3320	0.9409	−1.40	−0.1031
6	RNA25%	13.45	0.8831	0.0493	0.6404	−0.0152	0.8988	0.3486	0.9396	−1.99	0.1360
7	RNA10%	20.49	0.9877	0.1262	0.8380	−0.0448	0.9823	0.3663	0.9699	−5.16	0.7710
8	RU50%	13.84	0.8849	0.0524	0.6632	−0.0200	0.8417	0.3686	0.9213	−2.05	0.1610
9	RU25%	17.91	0.9662	0.0934	0.8680	−0.0349	0.9604	0.3655	0.9848	−3.78	0.5653
10	RU10%	25.28	0.9768	0.1888	0.8343	−0.0659	0.9877	0.3089	0.9999	−7.19	0.7615
11	RL127-50%	14.20	0.8121	0.0536	0.5233	−0.0202	0.8723	0.2808	0.9526	−2.09	−0.0958
12	RL127-25%	22.30	0.9384	0.1406	0.8141	−0.0408	0.9434	0.2631	0.9637	−5.51	0.6000
13	RL127-10%	29.58	0.8812	0.2751	0.7657	−0.1345	0.9123	0.0919 (0.8433)	0.9468 (0.9713)	−8.26	0.5356
14	RL68-50%	13.64	0.7956	0.0494	0.4804	−0.0184	0.7334	0.2504	0.9806	−2.00	−0.1471
15	RL68-25%	18.62	0.9285	0.0985	0.8298	−0.0377	0.9418	0.2700	0.9844	−3.88	0.4493
16	RL68-10%	23.43	0.9258	0.1579	0.8476	−0.0637	0.9504	0.2222	0.9962	−7.02	0.6805
17	RG44-50%	10.55	0.9602	0.0326	0.8507	−0.0122	0.9554	0.5451	0.9198	−1.33	0.4809
18	RG44-25%	13.09	0.9650	0.0455	0.8451	−0.0202	0.9830	0.5860	0.9386	−2.00	0.6182
19	RG44-10%	15.63	0.9496	0.0702	0.8310	−0.0271	0.9551	0.4103	0.9587	−2.72	0.4183
20	RPEG4-50%	13.49	0.9176	0.0430	0.8976	−0.0196	0.9398	0.3940	0.9478	−2.01	0.2782
21	RPEG4-25%	15.54	0.9600	0.0488	0.8961	−0.0252	0.9748	0.4113	0.9732	−2.72	0.4622
22	RPEG4-10%	22.74	0.9399	0.1124	0.8484	−0.0589	0.9483	0.2500	0.9950	−5.65	0.5972
23	RPEG6-50%	12.84	0.9577	0.0486	0.8621	−0.0183	0.9528	0.5410	0.9269	−1.95	0.5408
24	RPEG6-25%	15.07	0.9658	0.0662	0.8554	−0.0250	0.9594	0.4127	0.9793	−2.64	0.4851
25	RPEG6-10%	19.25	0.9046	0.1030	0.7058	−0.0394	0.8482	0.2778	0.9613	−4.01	0.3635
26	RPVP50%	16.76	0.8775	0.0950	0.8038	−0.0299	0.9738	0.2958	0.9661	−3.84	0.4985
27	RPVP25%	19.53	0.9360	0.1101	0.8459	−0.0441	0.9665	0.3139	0.9790	−4.09	0.4557
28	RPVP10%	32.86	0.9708	0.2235	0.5085	−0.0943	0.4726	0.0705 (0.3947)	0.3034 (0.9685)	−7.77	0.4879
29	RMann50%	8.07	0.9770	0.0195	0.7985	−0.0068	0.9007	0.4572	0.9904	−0.87	0.4736
30	RMann25%	9.56	0.8780	0.0248	0.6492	−0.0092	0.8469	0.3382	0.9838	−1.01	0.0158
31	RMann10%	14.16	0.8607	0.0546	0.6555	−0.0213	0.8643	0.3104	0.9656	−2.09	0.0446
32	RSorb50%	9.25	0.8933	0.0237	0.6855	−0.0087	0.8657	0.3499	0.9790	−0.98	0.0748
33	RSorb25%	9.97	0.8168	0.0264	0.5795	−0.0100	0.8226	0.3058	0.9802	−1.05	−0.1910
34	RSorb10%	13.49	0.8033	0.0486	0.5011	−0.0180	0.7444	0.2521	0.9835	−1.98	−0.1243

released. However, in cases where the total drug release in the entire dissolution time span was below 90%, data until the last sampling time, i.e., 120 min, were taken into consideration.

By and large, the Korsemeyer–Peppas model described drug release kinetics in the most befitting manner, barring only three formulations *viz*. RCA10%, RL127-10% and RPVP10% which showed very fast release (exhibiting more than 90% in 10 min). Except for RCA10%, which fitted to first-order kinetic model, the two other formulations did not fit mathematically to any other kinetic model. Studies, therefore, were subsequently repeated at shorter time intervals until 10 min, i.e., at 1, 2.5, 5, 7.5 and 10 min, for these formulations. Model fitting was reattempted until 90% of the drug released. The newer results have also been documented in parentheses in Table 4. After fitting the drug release data including these time points, these correlations were also found to be statistically significant with Korsemeyer–Peppas model.

Overall, the values of diffusional exponent '*n*', obtained from the slopes of the fitted Korsemeyer–Peppas model, ranged between 0.2222 and 0.8433. No clear trend was observed in the values of *n* among inter- and intra-drug–carrier systems. Except for a few cases (RL127-10%, RG44-50% RG44-25%, RPEG6-50%), all the solid dispersions tended to exhibit Fickian diffusional characteristics, as the corresponding values of *n* were lower than the standard value for declaring Fickian release behaviour, i.e., 0.4500 [22]. The two G44 formulations (RG44-50% and RG44-25%) showed *n* values marginally above 0.4500 construing slightly non-Fickian release behaviour. Similar non-Fickian behaviour has also been reported previously with the Gelucire dispersions of paracetamol and caffeine [50]. For the very fast dissolving RL127-10% formulation (release until 5 min = 90%), the value of *n* was observed to be 0.8433. Zero-order kinetics, fitted at these points, indicated statistically significant ($p < 0.05$) fit to this model ($r^2 = 0.9947$). The RPEG6-50% formulation also showed little non-Fickian behaviour. The non-Fickian behaviour of the dispersions formulated using L127 and PEG 6000 can be attributed to the gelling property of the former and the polymer relaxation with the latter.

Likewise, the formulations were observed to yield statistically valid correlations with the Higuchi and first-order models too. The results unequivocally point out the prevalence of diffusional mechanistic phenomena, in consonance with the results obtained while fitting Korsemeyer–Peppas model [8]. The Hixson-Crowell cube root model, in general, described the drug release data modestly with r^2 values ranging between 0.4804 and 0.8976.

3.4. Solid state characterization

To investigate the mechanistics of dissolution rate enhancement of most promising L127 systems, the following characterization studies were carried out for RL12710% solid dispersion:

3.4.1. Powder X-ray diffraction spectroscopy

Fig. 2 shows the diffraction spectra of pure RFX, treated RFX, the carrier, the solid dispersion and the corresponding physical mixture. The diffraction spectrum of the solid dispersion vis-à-vis pure drug, carrier and physical mixture indicates the changes produced in the drug crystal structure. The diffraction spectrum of pure RFX showed that the drug was of crystalline nature, as demonstrated by numerous distinct peaks observed at 2θ of 8.72°, 11.05°, 13.95°, 16.08°, 17.85°, 19.04°, 19.45°, 22.33°, 23.38°, 24.96°, and 28.23° (Fig. 2a). The treated sample of drug (melted and solidified) also showed similar superimposable diffraction spectrum indicating that the crystallinity of the drug was unaffected by the treatment (Fig. 2b). L127 showed two prominent peaks with the highest intensity at 2θ of 19.08° and 23.29° (Fig. 2c).

All the principal peaks from L127 and RFX were present in their physical mixture and solid dispersion, although with lower intensity. No new peaks could be observed, suggesting the absence of interaction between the drug and the carrier [51,53]. The prominent peaks from pure RFX at 2θ of 8.7°, 11.05°, 16.08°, 17.85°, 19.04°, 19.4°, 22.34°, 23.35°, 24.95°, and 28.18° were clearly seen at the same position in the physical mixture. Both the peaks of L127 existed in the physical mixture at their respective positions. However in solid dispersions, only some of the diffraction peaks of RFX at 2θ of 8.7°, 11.05°, 16.08°, 17.85°, 22.34°, 23.35° were observed with remarkably decreased intensity vis-à-vis the corresponding physical mixtures. The two peaks of RFX at 2θ of 19.04° and 19.45° and the peak of L127 at 2θ of 19.08° were seen as single diffraction peak at 19.23°. The second peak of L127 was also clearly visible at 2θ of 23.28°. The other diffraction peaks of the drug were indistinguishable from the spectral noise indicating changes in the crystal quality and structure. Relative reduction of diffraction intensity of RFX in L127 dispersion vis-à-vis physical mixtures at these angles suggests that either the quality of the crystals is reduced, or a change is induced in the crystal orientation, or some of the drug is still present in crystalline form [47,49,52]. The positions of diffraction peaks of L127 in the physical mixture and solid dispersion were quite superimposable, thus ruling out any plausibility of chemical interaction between these two components or existence of any other crystal morphology.

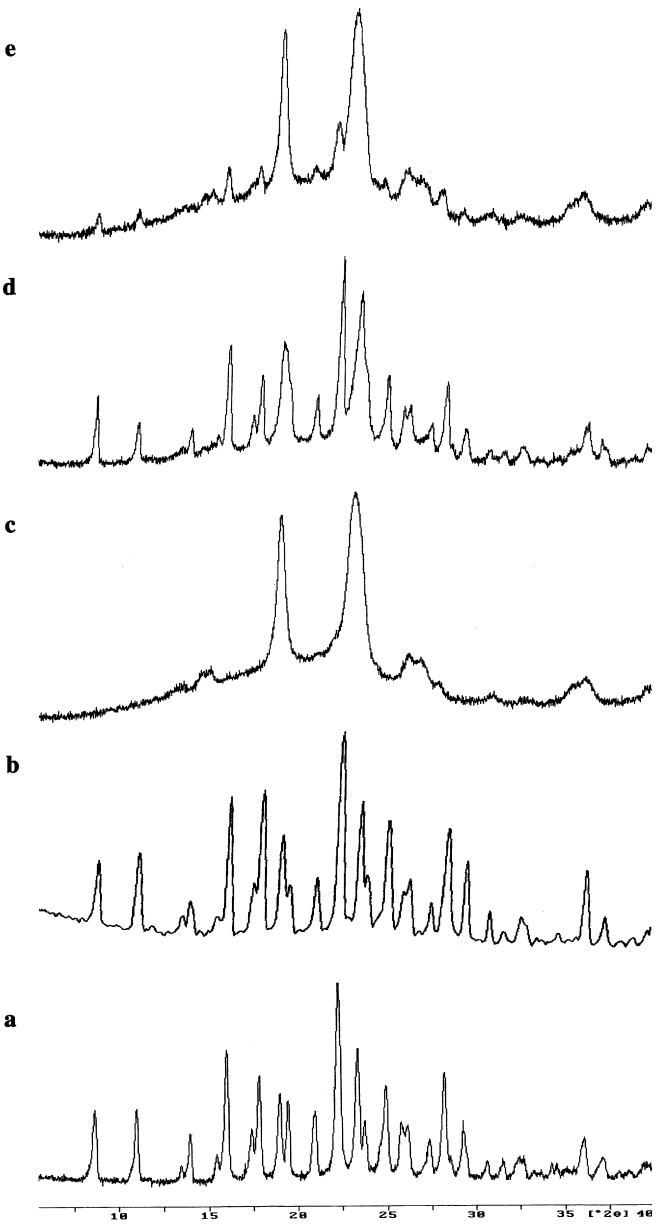

Fig. 2. X-ray diffraction patterns of (a) RFX; (b) treated RFX sample; (c) Lutrol® F127 (L127); (d) physical mixture of RFX-L127 binary systems with 10% w/w drug content; (e) solid dispersion of RFX-L127 binary system with 10% w/w drug content (RL12710%).

3.4.2. Fourier transform infrared spectroscopy

Fig. 3 shows the FTIR spectra of the drug, carrier, solid dispersion and the corresponding physical mixture. The results depicted that there was no significant change in the spectrum of solid dispersion, as incorporation of RFX into the L127 did not modify the position of its functional groups. The absence of shifts in the wavenumbers of the FTIR peaks of the solid dispersion vis-à-vis the physical mixture indicates the lack of significant interaction

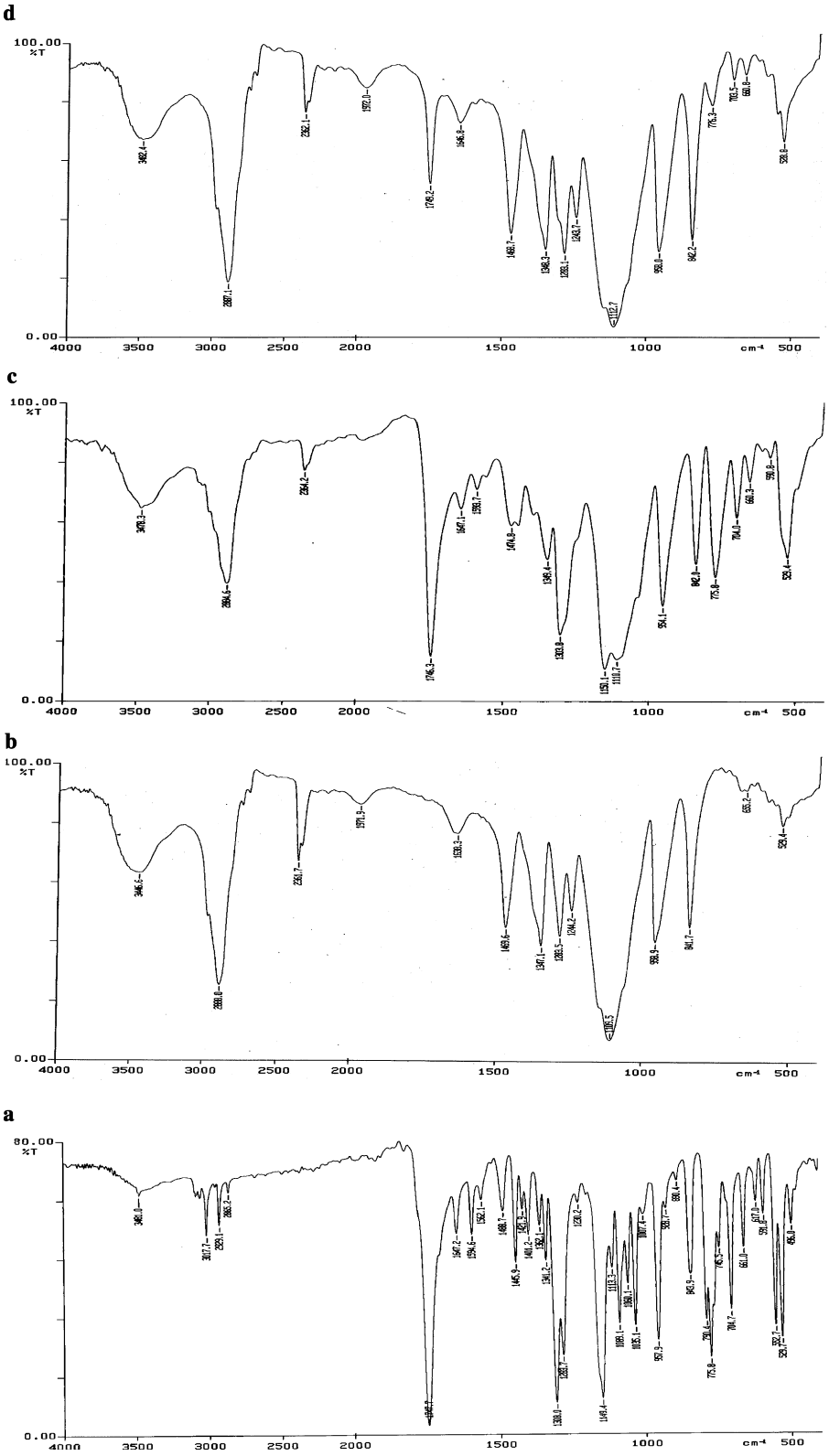

Fig. 3. FT-IR spectra of (a) RFX; (b) Lutrol® F127 (L127); (c) physical mixture of RFX-L127 binary systems with 10% w/w drug content; (d) solid dispersion of RFX-L127 binary system with 10% w/w drug content (RL12710%).

between the drug and the carrier in the solid dispersion [47,49]. Thus, these results ratify the absence of any well-defined interaction between RFX and the blockcopolymer as construed by the PXRD study.

3.4.3. Differential scanning calorimetry studies

Fig. 4 shows the DSC thermograms of RFX, L127, their physical mixture and the solid dispersion. The thermograms of RFX (Fig. 4a) and L127 (Fig. 4b) exhibit the

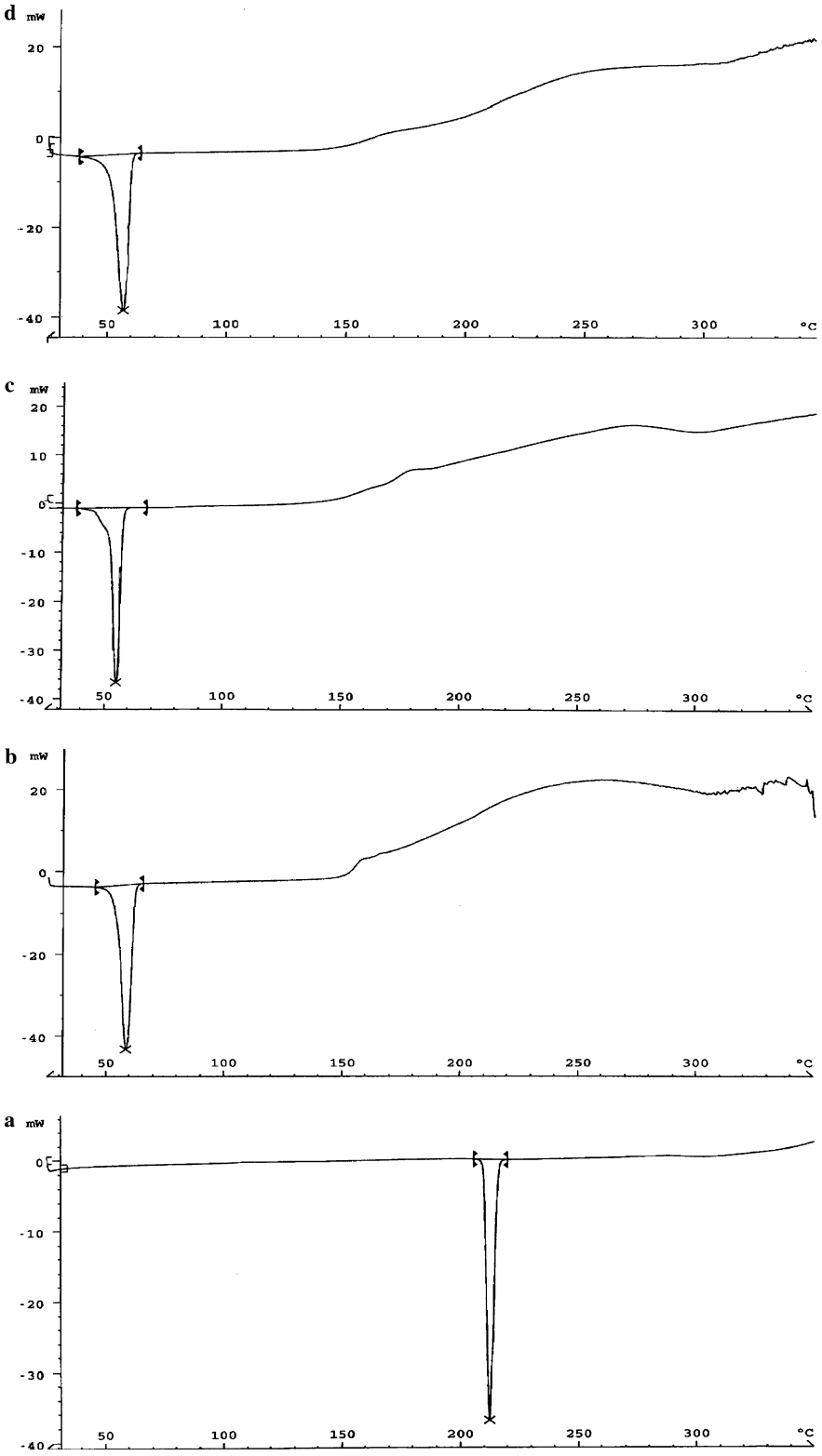

Fig. 4. DSC thermograms of (a) RFX; (b) Lutrol® F127 (L127); (c) physical mixture of RFX-L127 binary systems with 10% w/w drug content; (d) solid dispersion of RFX-L127 binary system with 10% w/w drug content (RL12710%).

corresponding single endothermic peaks at around 210.25 °C and 56.86 °C, respectively. The thermograms of both of the binary systems of RFX-L127, i.e., the physical mixture (Fig. 4c) and the solid dispersion (Fig. 4d) showed no endothermic peak corresponding to RFX. However, the diffraction peaks of crystalline RFX were observed in both of the PXRD spectra. It is quite probable that RFX might have dissolved in the molten carrier during DSC

measurement of the physical mixture and the solid dispersion. Therefore, only one endothermic peak was observed at around 53.47 °C (physical mixture) and 55.34 °C (solid dispersion), corresponding to the melting of L127. Analogous phenomena have also previously been reported by various researchers [40,51,54,55]. Almost similar thermal behaviour of the solid dispersion and the physical mixture corroborates the absence of any drug–carrier chemical interaction.

3.4.4. Scanning electron microscopy

Fig. 5a and b reveals that pure RFX and L127 exist in irregular crystalline shapes. The physical mixture of the drug and the carrier (Fig. 5c) shows the presence of drug in the crystalline form. On the other hand, the photomicrograph of the dispersion (Fig. 5d) shows the topological changes produced in the carrier particles. The carrier surface seems to be more porous in nature.

Solid state characterization studies revealed partial loss of drug crystallinity which can bring about significant change(s) in the drug dissolution rate. However, other factors like reduced particle size, increased surface area, and closer contact between the hydrophilic carrier and the drug may also be influential in enhancing drug solubility and/or dissolution rate observed with the solid dispersion particles.

4. Conclusions

Various water-soluble carriers investigated in the current study enhanced the solubility and dissolution characteristics of the poorly soluble drug to varying degrees, as a function of carrier concentration. The Korsemeyer–Peppas model most aptly fits the *in vitro* dissolution data and gives an insight into the possible drug release mechanisms invariably predominated by Fickian diffusion. Solid state characterization studies revealed that the drug crystallinity played pivotal role in governing the solubility characteristics of the drug. The results obtained with various carriers in the current studies can be extrapolated to other poorly

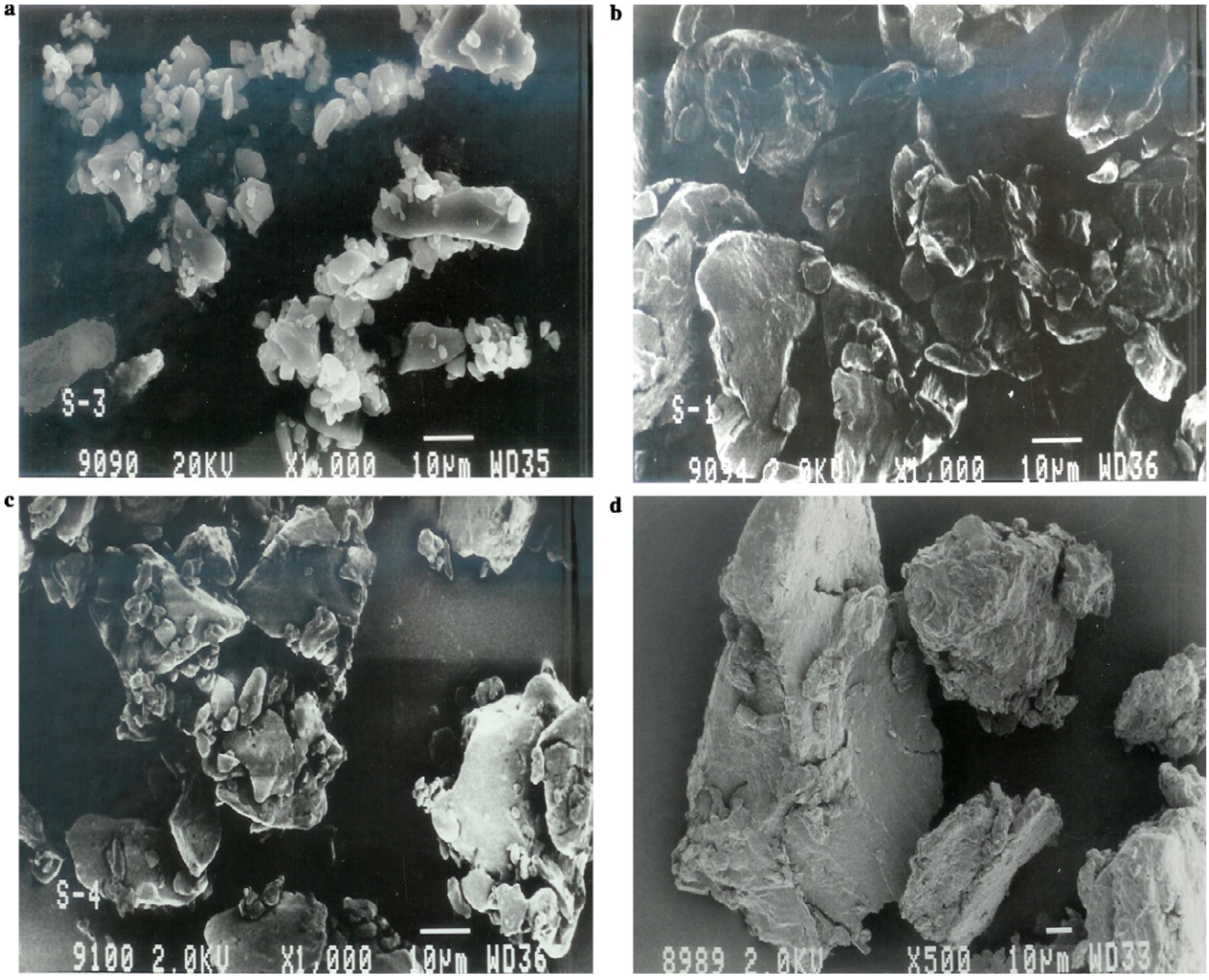

Fig. 5. Scanning electron microphotographs of (a) rofecoxib (RFX); (b) Lutrol® F127 (L127); (c) physical mixture of RFX-L127 binary systems with 10% w/w drug content; (d) solid dispersion of RFX-L127 binary system with 10% w/w drug content (RL12710%).

soluble BCS class II drugs too, where enhancement of *in vitro* drug solubility correlates well with improvement in their *in vivo* oral absorption. This can eventually alleviate the problems of delayed and inconsistent rate of drug absorption from gastrointestinal tract.

Acknowledgements

The authors are thankful to M/s Unichem Laboratories, India, M/s BASF, Bangalore, India, and M/s Gattefosse Ltd., France, for the gift samples of rofecoxib, Lutrols (F127 and F68), and Gelucire 44/14, respectively. The expert technical help rendered by Mr. M.L. Sharma and Mr. Navtej Singh during SEM studies, and Mr. Jagtar Singh for PXRD studies is duly acknowledged. The Council of Scientific and Industrial Research, New Delhi, India, is duly acknowledged for providing financial assistance to Ms. Naveen Ahuja for conducting the doctoral research under the guidance of Dr. Bhupinder Singh.

References

[1] G.L. Amidon, H. Lennernäs, V.P. Shah, J.R. Crison, A theoretical basis for a biopharmaceutic drug classification: the correlation of in vitro drug product dissolution and in vivo bioavailability, Pharm. Res. 12 (1995) 413–420.
[2] C. Leuner, J. Dressman, Improving drug solubility for oral delivery using solid dispersions, Eur. J. Pharm. Biopharm. 50 (2000) 47–60.
[3] C. Lipinski, Poor aqueous solubility – an industry wide problem in drug delivery, Am. Pharm. Rev. 5 (2002) 82–85.
[4] J. Hu, K.P. Johnston, R.O. Williams III, Rapid dissolving high potency danazol powders produced by spray freezing into liquid process, Int. J. Pharm. 271 (2004) 145–154.
[5] US FDA, Guidance for Industry, Waiver of in vivo bioavailability and bioequivalence studies for immediate release solid oral dosage forms based on a biopharmaceutics classification system., Center for Drug Evaluation and Research, Fishers Lane, Rockville, MD August (2000) pp. 1–13.
[6] D.A. Wyatt, Taking poorly water soluble compounds through discovery, in: Recent Advances in the Formulations and Development of Poorly Soluble Drugs, Bulletin Technique Gattefossé, 1999, pp. 31–39.
[7] D.Q.M. Craig, The use of self-emulsifying systems as a means of improving drug delivery, in: Bulletin Technique Gattefossé, 1993, pp. 21–31.
[8] M.J. Habib, Pharmaceutical Solid Dispersion Technology, Technomic Publishing, Lancaster, Pennysylvania, 2001, pp. 7–36.
[9] A.T.M. Serajuddin, Solid dispersion of poorly water soluble drugs: early promises, subsequent problems, and recent breakthroughs, J. Pharm. Sci. 88 (1999) 1058–1066.
[10] W.N. Charman, Lipids, lipophilic drugs, and oral drug delivery: some emerging concepts, J. Pharm. Sci. 89 (2000) 967–978.
[11] N. Ahuja, A. Singh, B. Singh, Rofecoxib: an update on physicochemical, pharmaceutical, pharmacodynamic and pharmacokinetic aspects, J. Pharm. Pharmacol. 55 (2003) 859–894.
[12] M. Depré, E. Ehrich, A. Van Hecken, I. De Lepeleire, A. Dallob, P. Wong, A. Porras, B.J. Gertz, P.J. De Schepper, Pharmacokinetics, COX-2 specificity, and tolerability of supratherapeutic doses of rofecoxib in humans, Eur. J. Clin. Pharmacol. 56 (2000) 167–174.
[13] N. Seedher, S. Bhatia, Solubility enhancement of COX-2 inhibitors using various solvent systems, AAPS Pharm. Sci. Techmol. 4 (2003) E33.
[14] S. Rawat, S.K. Jain, Rofecoxib-beta-cyclodextrin inclusion complex for solubility enhancement, Pharmazie 58 (2003) 639–641.
[15] C. Liu, K.G. Desai, C. Liu, H.J. Park, Enhancement of dissolution rate of rofecoxib using solid dispersions with urea, Drug Dev. Res. 63 (2004) 181–189.
[16] S. Baboota, M. Dhaliwal, K. Kohli, Physicochemical characterization, in vitro dissolution behavior, and pharmacodynamic studies of rofecoxib-cyclodextrin inclusion compounds. Preparation and properties of rofecoxib hydroxypropyl beta-cyclodextrin inclusion complex: a technical note, AAPS Pharm. Sci. Technol. 6 (2005) E83–E90.
[17] C. Liu, K.G. Desai, Characteristics of rofecoxib-polyethylene glycol 4000 solid dispersions and tablets based on solid dispersions, Pharm. Dev. Technol. 10 (2005) 467–477.
[18] T. Higuchi, K.A. Connors, Phase solubility techniques, Adv. Anal. Chem. Instr. 4 (1965) 117–212.
[19] B. Singh, T. Kaur, S. Singh, Correction of raw dissolution data for loss of drug and volume during sampling, Indian J. Pharm. Sci. 59 (1997) 196–199.
[20] K.A. Khan, The concept of dissolution efficiency, J. Pharm. Pharmacol. 27 (1975) 48–49.
[21] T. Higuchi, Mechanism of sustained-action medication: theoretical analysis of rate of release of solid drugs dispersed in solid matrices, J. Pharm. Sci. 52 (1963) 1145–1149.
[22] R.W. Korsemeyer, R. Gurney, E. Doelker, P. Buri, N.A. Peppas, Mechanisms of solute release from porous hydrophilic polymers, Int. J. Pharm. 15 (1983) 25–35.
[23] W.A. Ritschel, Biopharmaceutic and pharmacokinetic aspects in the design of controlled release peroral drug delivery systems, Drug Dev. Ind. Pharm. 15 (1989) 1073–1103.
[24] B. Singh, S. Singh, A comprehensive computer program for the study of drug release kinetics from compressed matrices, Indian J. Pharm. Sci. 60 (1998) 358–362.
[25] M. Cirri, P. Mura, A.M. Rabasco, J.M. Ginés, J.R. Moyano, M.L. Gònzalez-Rodrìguez, Characterization of ibuproxam binary and ternary dispersions with hydrophilic carriers, Drug Dev. Ind. Pharm. 30 (2004) 65–74.
[26] M. Shahjahan, R.P. Enever, Investigation of the nature of the interaction of nitrofurazone with urea, Int. J. Pharm. 82 (1992) 229–232.
[27] H. Sekikawa, M. Nakano, T. Arita, Inhibitory effects of polyvinylpyrrolidone on the crystallization of drugs, Chem. Pharm. Bull. 26 (1978) 118–126.
[28] O.I. Corrigan, R.F. Timoney, The influence of polyethylene glycols on the dissolution properties of hydroflumetiazide, Pharm. Acta Helv. 51 (1976) 268–271.
[29] W.L. Chiou, Pharmaceutical applications of solid dispersions systems: X-ray diffraction and aqueous solubility studies on griseofulvine-polyethylene glycol 6000 systems, J. Pharm. Sci. 66 (1977) 989–991.
[30] I. Rácz, Physicochemical interactions encountered in the course of drug product preparation, in: Drug Formulation, Wiley J and Sons, New York, 1989, pp. 212–242.
[31] A.V. Kabanov, P. Lemieux, S. Vinogradov, V. Alakhov, Pluronic® block copolymers: novel functional molecules for gene therapy, Adv. Drug Deliv. Rev. 54 (2002) 223–233.
[32] J.B. Dressman, H. Lennernäs (Eds.), Oral drug absorption: Prediction and assessment, Marcel Dekker, New York, 2000 (B. Singh, N. Ahuja, Book Review on Oral Drug Absorption: Prediction and Assessment, Pharma Times, 2001, 33 (12), 10; Indian J. Pharm. Ed., 2001, 63, 321).
[33] A.T.M. Serajuddin, P.C. Sheen, D. Mufson, D.F. Bernstein, M.A. Augustine, Effect of vehicle amphiphilicity on the dissolution and bioavailability of a poorly water-soluble drug from solid dispersions, J. Pharm. Sci. 77 (1988) 414–417.
[34] A.T.M. Serajuddin, P.C. Sheen, M.A. Augustine, Improved dissolution of poorly water-soluble drug from solid dispersions in polyethylene: Polysorbate 80 mixture, J. Pharm. Sci. 79 (1990) 463–464.
[35] M. Fawzi, E. Davison, M. Tute, Rationalization of drug complexation in aqueous solution by use of huckel frontier molecular orbitals, J. Pharm. Sci. 69 (1980) 104–105.

[36] S. Feldman, M. Gibaldi, Effect of urea on solubility: role of water structure, J. Pharm. Sci. 56 (1967) 370–375.
[37] S. Bogdanova, D. Sidzhakova, V. Karaivanova, S. Georgieva, Aspects of the interactions between indomethacin and nicotinamide in solid dispersions, Int. J. Pharm. 163 (1998) 1–10.
[38] M.P. Summers, R.P. Enever, Preparation and properties of solid dispersion system containing citric acid and primidone, J. Pharm. Sci. 65 (1976) 1613–1617.
[39] M.P. Summers, Glass formation in barbiturates and solid dispersion systems of barbiturates with citric acid, J. Pharm. Sci. 67 (1978) 1606–1610.
[40] G. van den Mooter, P. Augustijns, N. Blaton, R. Kinget, Physicochemical characterization of solid dispersions of temazepam with polyethylene glycol 6000 and PVP K30, Int. J. Pharm. 164 (1998) 67–80.
[41] A.M. Abdul-Fattah, H.N. Bhargava, Preparation and in vitro evaluation of solid dispersions of halofantrine, Int. J. Pharm. 235 (2002) 17–33.
[42] K. Itoh, Y. Tozuka, T. Oguchi, K. Yamamoto, Improvement of physicochemical properties of N-4472: Part I. Formulation design by using self-microemulsifying system, Int. J. Pharm. 238 (2002) 153–160.
[43] S.A. Barker, S.P. Yap, K.H. Yuen, C.P. McCoy, J.R. Murphy, D.Q.M. Craig, An investigation into the structure and bioavailability of α-tocopherol dispersions in Gelucire 44/14, J. Control. Release 91 (2003) 477–488.
[44] K. Yamashita, T. Nakate, K. Okimoto, A. Ohike, Y. Tokunaga, R. Ibuki, K. Higaki, T. Kimura, Establishment of new preparation method for solid dispersion formulation of tacrolimus, Int. J. Pharm. 267 (2003) 79–91.
[45] K. Okimoto, M. Miyake, R. Ibuki, M. Yasumura, N. Ohnishi, T. Nakai, Dissolution mechanism and rate of solid dispersion particles of nifedipine with hydroxypropylmethylcellulose, Int. J. Pharm. 159 (1997) 85–93.
[46] N. Kohri, Y. Yamayoshi, H. Xin, K. Iseki, N. Sato, S. Todo, K. Miyazaki, Improving the oral bioavailability of albendazole in rabbits by the solid dispersion technique, J. Pharm. Pharmacol. 51 (1999) 159–164.
[47] S.R. Vippagunta, K.A. Maul, S. Tallavajhala, D.J.W. Grant, Solid-state characterization of nifedipine solid dispersions, Int. J. Pharm. 236 (2002) 111–123.
[48] S.Y. Lin, Y. Kawashima, The influence of three poly(-oxyethylene)poly(oxypropylene) surface-active block copolymers on the solubility behavior of indomethacin, Pharm. Acta Helv. 60 (1985) 339–344.
[49] H. Valizadeh, A. Nokhodchi, N. Qarakhani, P. Zakeri-Milani, S. Azarmi, D. Hassanzadeh, R. Löbenberg, Physicochemical characterization of solid dispersions of indomethacin with PEG 6000, Myrj 52, lactose, sorbitol, dextrin, and Eudragit® E100, Drug Dev. Ind. Pharm. 30 (2004) 303–317.
[50] N. Khan, D.Q.M. Craig, The influence of drug incorporation on the structure and release properties of solid dispersions in lipid matrices, J. Control. Release 93 (2003) 355–368.
[51] F. Damian, N. Blaton, L. Naesens, J. Balzarini, R. Kinget, P. Augustijns, G. Van den Mooter, Physicochemical characterization of solid dispersions of the antiviral agent UC-781 with polyethylene glycol 6000 and Gelucire 44/14, Eur. J. Pharm. Sci. 10 (2000) 311–322.
[52] G.V. Betageri, K.R. Makarla, Enhancement of dissolution of glyburide by solid dispersion and lyophilization techniques, Int. J. Pharm. 126 (1995) 155–160.
[53] B.C. Hancock, G. Zografi, Characteristic and significance of the amorphous state in pharmaceutical systems, J. Pharm. Sci. 86 (1997) 1–12.
[54] M. Guyot, F. Fawaz, J. Bildet, F. Bonini, A.M. Lagueny, Physicochemical characterisation and dissolution of norfloxacin/cyclo-dextrin inclusion compounds and PEG solid dispersions, Int. J. Pharm. 123 (1995) 53–63.
[55] D.Q.M. Craig, J.M. Newton, Characterisation of polyethylene glycols using differential scanning calorimetry, Int. J. Pharm. 74 (1991) 33–41.